

SAND REPORT

SAND 2002-0138

Unlimited Release

Printed January 2002

Sweeping Gas Membrane Desalination Using Commercial Hydrophobic Hollow Fiber Membranes

Lindsey R. Evans and James E. Miller

Prepared by
Sandia National Laboratories
Albuquerque, New Mexico 87185 and Livermore, California 94550

Sandia is a multiprogram laboratory operated by Sandia Corporation,
a Lockheed Martin Company, for the United States Department of
Energy under Contract DE-AC04-94AL85000.

Approved for public release; further dissemination unlimited.



Issued by Sandia National Laboratories, operated for the United States Department of Energy by Sandia Corporation.

NOTICE: This report was prepared as an account of work sponsored by an agency of the United States Government. Neither the United States Government, nor any agency thereof, nor any of their employees, nor any of their contractors, subcontractors, or their employees, make any warranty, express or implied, or assume any legal liability or responsibility for the accuracy, completeness, or usefulness of any information, apparatus, product, or process disclosed, or represent that its use would not infringe privately owned rights. Reference herein to any specific commercial product, process, or service by trade name, trademark, manufacturer, or otherwise, does not necessarily constitute or imply its endorsement, recommendation, or favoring by the United States Government, any agency thereof, or any of their contractors or subcontractors. The views and opinions expressed herein do not necessarily state or reflect those of the United States Government, any agency thereof, or any of their contractors.

Printed in the United States of America. This report has been reproduced directly from the best available copy.

Available to DOE and DOE contractors from
U.S. Department of Energy
Office of Scientific and Technical Information
P.O. Box 62
Oak Ridge, TN 37831

Telephone: (865)576-8401
Facsimile: (865)576-5728
E-Mail: reports@adonis.osti.gov
Online ordering: <http://www.doe.gov/bridge>

Available to the public from
U.S. Department of Commerce
National Technical Information Service
5285 Port Royal Rd
Springfield, VA 22161

Telephone: (800)553-6847
Facsimile: (703)605-6900
E-Mail: orders@ntis.fedworld.gov
Online order: <http://www.ntis.gov/ordering.htm>



Sweeping Gas Membrane Desalination Using Commercial Hydrophobic Hollow Fiber Membranes

Lindsey R. Evans and James E. Miller
Materials Chemistry Department
Sandia National Laboratories
P.O. Box 5800
Albuquerque, NM 87185-1349

Abstract

Water shortages affect 88 developing countries that are home to half of the world's population. In these places, 80-90% of all diseases and 30% of all deaths result from poor water quality. Furthermore, over the next 25 years, the number of people affected by severe water shortages is expected to increase fourfold. Low cost methods of purifying freshwater, and desalting seawater are required to contend with this destabilizing trend.

Membrane distillation (MD) is an emerging technology for separations that are traditionally accomplished via conventional distillation or reverse osmosis. As applied to desalination, MD involves the transport of water vapor from a saline solution through the pores of a hydrophobic membrane. In sweeping gas MD, a flowing gas stream is used to flush the water vapor from the permeate side of the membrane, thereby maintaining the vapor pressure gradient necessary for mass transfer. Since liquid does not penetrate the hydrophobic membrane, dissolved ions are completely rejected by the membrane. MD has a number of potential advantages over conventional desalination including low temperature and pressure operation, reduced membrane strength requirements, compact size, and 100% rejection of non-volatiles.

The present work evaluated the suitability of commercially available technology for sweeping gas membrane desalination. Evaluations were conducted with Celgard Liqui-Cel[®] Extra-Flow 2.5X8 membrane contactors with X-30 and X-40 hydrophobic hollow fiber membranes. Our results show that sweeping gas membrane desalination systems are capable of producing low total dissolved solids (TDS) water, typically 10 ppm or less, from seawater, using low grade heat. However, there are several barriers that currently prevent sweeping gas MD from being a viable desalination technology. The primary problem is that large air flows are required to achieve significant water yields, and the costs associated with transporting this air are prohibitive. To overcome this barrier, at least two improvements are required. First, new and different contactor geometries are necessary to achieve efficient contact with an extremely low pressure drop. Second, the temperature limits of the membranes must be increased. In the absence of these improvements, sweeping gas MD will not be economically competitive. However, the membranes may still find use in hybrid desalination systems.

Table of Contents

1. Desalination Basics	6
2. Membrane Distillation Basics	11
3. Hollow Fiber Membrane Contactor Evaluation	14
4. Hollow Fiber Membrane Desalination System Evaluation	23
5. Conclusions and Recommendations	31
Acknowledgements	32
References	32

List of Figures

Figure 1. Schematic diagram of a basic multi-stage flash desalination process	6
Figure 2. Schematic diagram of a basic multi-effect evaporation desalination process ..	7
Figure 3. Schematic diagram of a single stage mechanical vapor compression desalination process	7
Figure 4. Schematic diagram of reverse osmosis desalination system	8
Figure 5. Methods employed in a membrane distillation scheme	12
Figure 6. Schematic diagram of hollow fiber membrane cartridge with counter current sweeping gas flow	14
Figure 7. Schematic of the basic membrane module test setup	15
Figure 8. Water production rate as a function of airflow and water temperature for the Celgard X-30 membrane contactor	16
Figure 9. Water production rate as a function of airflow and water temperature for the Celgard X-40 membrane contactor	17
Figure 10. Effect of air inlet temperature on water yield using a Celgard X-30 (and X-40) contactor	18
Figure 11. Data from Figure 10 (X-30 only) replotted to show that membrane contactor acts as an efficient counter-current heat exchanger	19
Figure 12. Water yield compared to the theoretical yield based on air saturation at the air exit temperature for the X-30 contactor	20
Figure 13. Water yield compared to the theoretical yield based on air saturation at the water inlet temperature for the X-30 contactor	20

Figure 14. Water yield compared to the theoretical yield based on air saturation at the air exit temperature for the X-40 contactor 21

Figure 15. Water yield compared to the theoretical yield based on air saturation at the water inlet temperature for the X-40 contactor 21

Figure 16. Schematic of the stand-alone membrane module test setup 23

Figure 17. Schematic depiction of an MD system operating with a bank of contactors 25

Figure 18. Proposed scheme for more efficient heat utilization in sweeping gas MD .. 27

Figure 19. Saturation humidity of air as a function of temperature – adapted from “Perry’s Chemical Engineering Handbook, 6th edition” 28

Figure 20. Multicontactor configuration for minimizing air flow requirements 30

List of Tables

Table 1. Energy Use for Desalination 9

Table 2. Desalination Costs 9

Table 3: Celgard Liqui-Cel[®] Membrane Properties 14

Table 4: Temperature profiles across the X-40 membrane at various air and water flows 24

Table 5. Results of experimental simulation of system depicted in Figure 17 26

Table 6. Thermal and saturation efficiency for system depicted in Figure 17 26

Table 7. Approximate operating costs for low-pressure air blowers used in a 1000 gallon/day sweep gas MD system (\$0.10/kWhr basis) 30

1. Desalination Basics

Water shortages affect 88 developing countries that are home to half of the world's population. In these places, 80-90% of all diseases and 30% of all deaths result from poor water quality [1]. Furthermore, over the next 25 years, the number of people affected by severe water shortages is expected to increase fourfold [2]. Low cost methods of purifying freshwater, and desalting seawater are required to contend with this destabilizing trend.

Currently, about 80% of the world's desalination capacity is provided by two technologies: Multi-stage flash (MSF), and reverse osmosis (RO) [3]. MSF units are widely used in the Middle East (particularly in Saudi Arabia, the United Arab Emirates, and Kuwait) and they account for over 40% of the world's desalination capacity [3]. MSF is a distillation (thermal) process that involves evaporation and condensation of water. The evaporation and condensation steps are coupled in MSF so that the latent heat of evaporation is recovered for reuse (Figure 1). To maximize water recovery, each stage of an MSF unit operates at a successively lower pressure. A key design feature of MSF systems is bulk liquid boiling. This alleviates problems with scale formation on heat transfer tubes. In the Persian Gulf region, large MSF units are often coupled with steam or gas turbine power plants for better utilization of the fuel energy. Steam produced at high temperature and pressure by the fuel is expanded through the turbine to produce electricity. The low to moderate temperature and pressure steam exiting the turbine is used to drive the desalination process [4-6]. A performance ratio often applied to thermal desalination processes is the gained output ratio, defined as the mass of water product per mass of heating steam. A typical gained output ratio for MSF units is 8 [3,6,7]. A 20 stage plant has a typical heat requirement of 290 kJ/kg product [6].

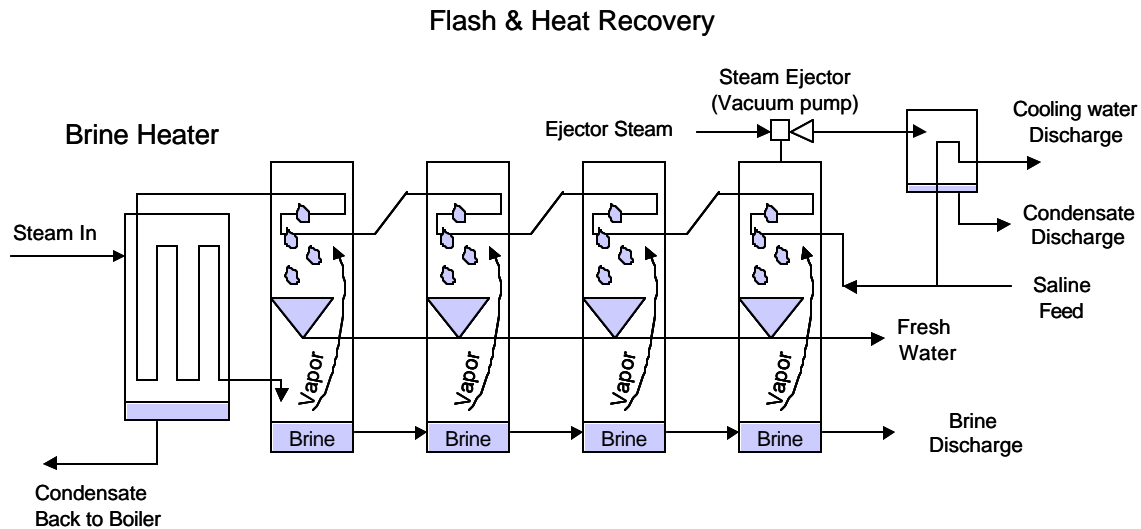


Figure 1. Schematic diagram of a basic multi-stage flash desalination process.

Multi-effect evaporation (MEE) is distillation process related to MSF (Figure 2). It is not yet widely used, but has gained attention due to the better thermal performance compared to MSF. In MEE, vapor from each stage is condensed in the next successive stage thereby giving up its heat to drive more evaporation. To increase the performance, each

stage is run at a successively lower pressure. Alternately, heat can be added to the vapor between stages, e.g. by mechanical (MVC, Figure 3) or thermal vapor compression (TVC). Hybrid MEE-TVC systems may have thermal performance ratios (similar to the gain ratio, energy used to evaporate water in all the stages/ first stage energy input) approaching 17 [3], while the combination of MEE with a lithium bromide/water absorption heat pump yielded a thermal performance ratio of 21 [8]. By themselves, vapor compression processes are particularly useful for small to medium installations [9].

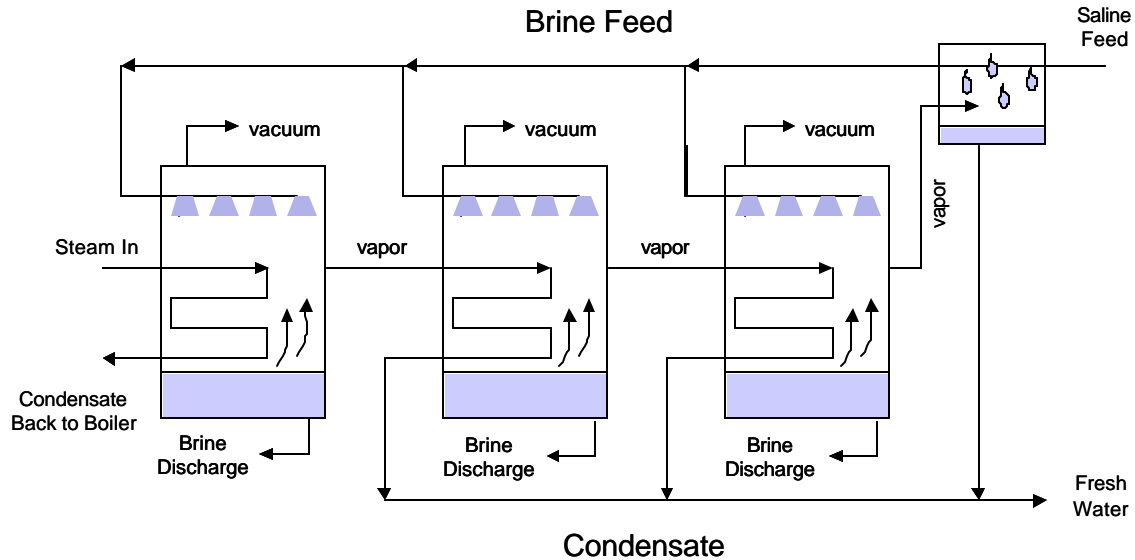


Figure 2. Schematic diagram of a basic multi-effect evaporation desalination process.

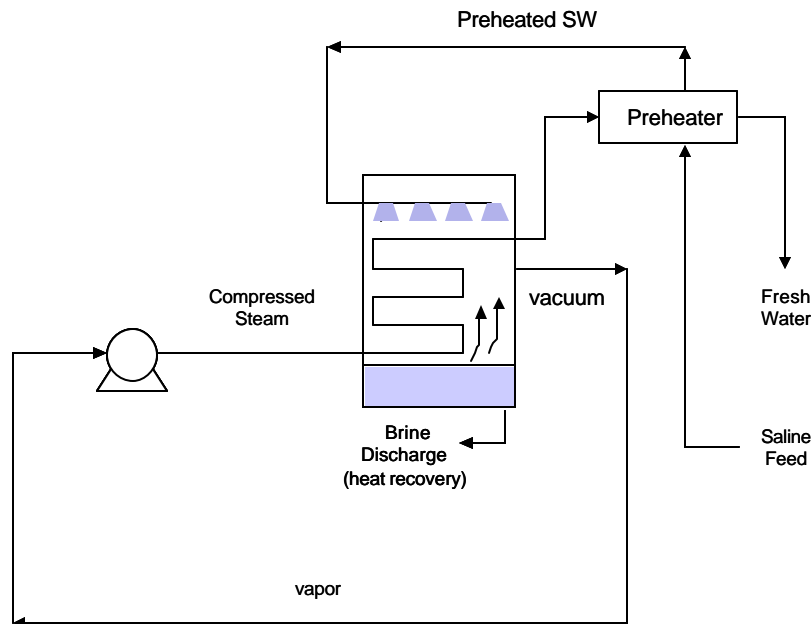


Figure 3. Schematic diagram of a single stage mechanical vapor compression desalination process.

RO is a non thermal membrane separation process that recovers water from a pressurized saline solution (Figure 4). The United States ranks second worldwide in desalination capacity, primarily relying on RO to treat brackish and surface water [5]. In essence, the membrane filters out the salt ions from the pressurized solution, allowing only the water to pass. RO post-treatment includes removing dissolved gasses (CO₂), and stabilizing the pH via the addition of Ca or Na salts. Pressurizing the saline water accounts for most of the energy consumed by RO. Since the pressure required to perform the separation is directly related to the salt concentration, RO is often the method of choice for brackish water, where only low to intermediate pressures are required. The operating pressure for brackish water systems ranges from 15 – 25 bar and for seawater systems from 54 to 80 bar (the osmotic pressure of seawater is about 25 bar) [9]. Since the pressure required to recover additional water increases as the brine stream is concentrated, the water recovery rate of RO systems tends to be low. A typical recovery value for a seawater RO system is 40% [6]. Large scale RO systems are now equipped with devices to recover the mechanical compression energy from the discharged concentrated brine stream. In these plants, the energy required for seawater desalination has been reported to be as low as 11 kJ/kg product [9]. RO membranes are sensitive to pH, oxidizers, a wide range of organics, algae, bacteria and of course particulates and other foulants [5]. Therefore, pretreatment of the feed water is an important consideration and can a significant impact on the cost of RO [7], especially since all the feed water, even the 60% that will eventually be discharged, must be pretreated before being passed to the membrane.

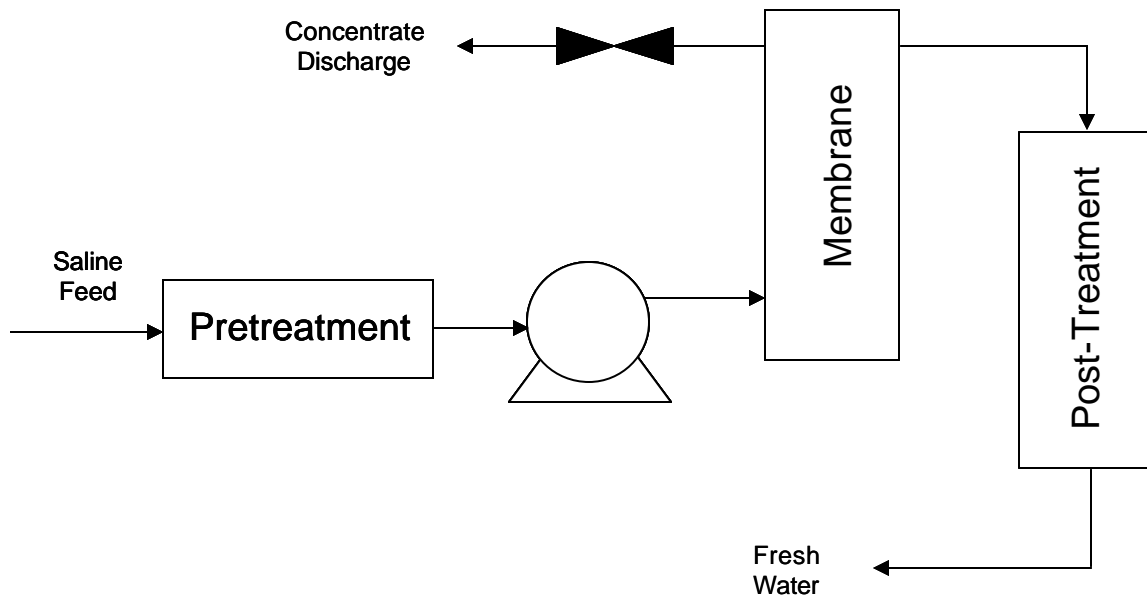


Figure 4. Schematic diagram of reverse osmosis desalination system.

The theoretical minimum energy for desalination is calculated to be 3-7 kJ/kg water [6,10,11]. Although this number can be arrived at in a number of ways, it is perhaps easiest to think of this number as the energy associated with the process of salt dissolution. For comparison Table 1 provides literature values for the energy requirements of different desalination processes. Table 2 presents the costs reported for water produced by different methods.

Table 1. Energy Use for Desalination (kJ/kg fresh water – divide by 3.6 for kWhr/m³)

Reference	Seawater RO	MSF	VC
A	61	299	
B	15-28	95	
C	27	230	
D	23-30	290	
E	18-22 (11 brackish)	216-288	
F	11		25-43
G	15-28		29-39
H			22-29
I			14-29
J			25-36
K			26
L			37

- A. R.V. Wahlgren, Wat. Res. 35 (2001) 1.
 B. L. Awerbuch, Proc. IDA World Congress on Desalination and Water Reuse, Madrid, 4 (1997)181.
 C. M.A. Darwish; N.M. Al-Najem, Applied Thermal Engineering 20 (2000) 399.
 D. K.S. Speigler and Y.M. El-Sayed, A Desalination Primer, Balaban Desalination Publications, Santa Maria Imbaro, Italy (1994).
 E. K.E. Thomas, NREL report TP-440-22083 (1997).
 F. O.K. Buros, "The ABCs of Desalting, Second ed." International Desalination Association, Topsfield, Mass, 2000.
 G. L. Awerbuch, Proc. Intl. Symposium on Desalination of Seawater with Nuclear Energy, IAEA (1997) 413.
 H. H.M. Ettouney, H.T. El-Dessouky, I. Alatiqi, Chemical Engineering Progress, September 1999, 43.
 I. F. Mandani, H. Ettouney, H. El-Dessouky, Desalination 128 (2000) 161.
 J. F. Al-Juwayhel, H. El-Dessouky, H. Ettouney, Desalination (1997) 253.
 K. S.E. Aly, Energy Conversion and Management 40 (1999) 729.
 L. J.M. Veza, Desalination 101 (1995) 1.

Table 2. Desalination Costs (\$/m³ fresh water – multiply by 3.8 for \$/1000 gal)

Reference	Seawater RO	Brackish RO	MSF	MEE	VC
A	0.45-0.92	0.20-0.35	1.10-1.50	0.46-85	0.87-0.92
B	0.72-0.93		0.80	0.45	
C	0.68		0.89		0.27-0.56
D	0.45-0.85		0.70-0.75		
E	1.54	0.35			
F	1.50	0.34-0.64			
G	1.31-2.68				
H			1.86	1.49	
I	1.06			1.35	
J	1.25				
K	1.22				
L		0.18-0.56			
M					0.46

- A. R. Semiat, Water International 25 (2000) 54.

- B.** J. Bednarski, M. Minamide, O.J. Morin, Proc., IDA World Congress on Desalination and Water Science, Madrid, 1 (1997) 227.
- C.** G. Kronenberg, Proc., IDA World Congress on Desalination and Water Science, Abu Dhabi, 3 (1995) 459.
- D.** O.K. Buros, "The ABCs of Desalting, Second ed." International Desalination Association, Topsfield, Mass, 2000.
- E.** F.I.A. Cortes and A.M. Dominguez, Ingenieria Hidraulica En Mexico 15 (2000) 27.
- F.** K.S. Speigler and Y.M. El-Sayed, A Desalination Primer, Balaban Desalination Publications, Santa Maria Imbaro, Italy (1994).
- G.** R.V. Wahlgren, Wat. Res. 35 (2001) 1.
- H.** O.J. Morin, Desalination 93 (1993) 343.
- I.** G. Hess and O.J. Morin, Desalination 87 (1992) 55.
- J.** E. Drioli, F. Lagana, A. Criscuoli, G. Barbieri, Desalination 122 (1999) 141.
- K.** T.M. Leahy, Int. Desalination and Water Reuse 7 (1998) 2832.
- L.** J.S. Taylor and E.P. Jacobs in Water Treatment Membrane Processes, Mallevalle, Odendaal, Wiesner, eds. McGraw-Hill, New York (1996).
- M.** Z. Zimmerman, Desalination 96 (1994) 51.

Despite the fact that MSF is a very mature technology (50 years), Table 1 shows that the energy consumption is still at least 30 times the theoretical minimum energy to separate salt from seawater. RO is a slightly newer technology (30 years), and with improvements in energy recovery, it now consumes only 4-20 times the theoretical energy (using the conservative 3 kJ/kg number), indicating it is closer to being a thermodynamically reversible process than the distillation methods. It is important to consider however that RO consumes energy in the form of electricity. On the other hand, MSF uses heat (or fuel) more directly. The conversion of thermal energy to electrical energy is only about 35% efficient. Therefore, on a fuel basis, RO consumes 12-60 times the theoretical energy, making it somewhat comparable to MSF.

2. Membrane Distillation Basics

Membrane distillation (MD) is an emerging alternate technology for separations that are traditionally accomplished via conventional distillation or reverse osmosis. Specifically, membrane distillation refers to membrane separations processes with the following characteristics: 1) the membrane is porous 2) the membrane is not wetted by the process liquids 3) no capillary condensation takes place in the pores of the membrane 4) the membrane does not alter the vapor-liquid equilibrium of the components of the process liquids 5) at least one side of the membrane is in contact with the process liquid 6) the driving force of membrane operation is a partial pressure gradient in the liquid phase [12]. Pervaporation is a related technology that may employ wetted membranes. MD has a number of potential advantages over conventional desalination processes such as evaporation and reverse osmosis [13]. These include: 1) low operating temperature, 2) low operating pressure, 3) reduced membrane mechanical strength requirements, 4) less vapor space requirements, and 5) potentially 100% separation of solutes and non-volatiles.

As applied to desalination then, MD involves the transport of water vapor from a liquid saline stream through the pores of a hydrophobic membrane. Since the hydrophobic membrane is not wetted, water vapor passes through the membrane pores but the aqueous solution is prevented from passing through the pores. Water vapor (and any other volatiles present) transfer across the hydrophobic membrane and are condensed or removed as a vapor from the permeate side of the membrane module. Since liquid does not transport across hydrophobic membrane, dissolved ions (with virtually no vapor pressure) are completely rejected by the membrane. A variety of methods have been employed to impose a vapor pressure difference across the membranes for MD [13]. As shown in Figure 5, the four methods are:

1. Direct contact MD - This configuration is the simplest to mode of MD. In this arrangement vapor from a feed stream traverses the membrane and condenses directly into a solution flowing on the permeate side of the membrane. If temperature is used to provide the vapor pressure gradient, heat transfer from the heated feed to the product (temperature polarization) can be a limitation.
2. Air gap MD - In this case, an air gap separates the hydrophobic membrane from a cool condensing surface. This is one of the most versatile methods.
3. Sweeping gas MD - A flowing gas is used to sweep the vapor out of the membrane permeate side, thereby maintaining the gradient necessary for transport. This is particularly useful for removing volatile components or dissolved gasses from liquid streams.
4. Vacuum MD – A vacuum is maintained on the permeate side to facility vapor transport across the membrane. Also useful for removing volatile components or degassing liquids.

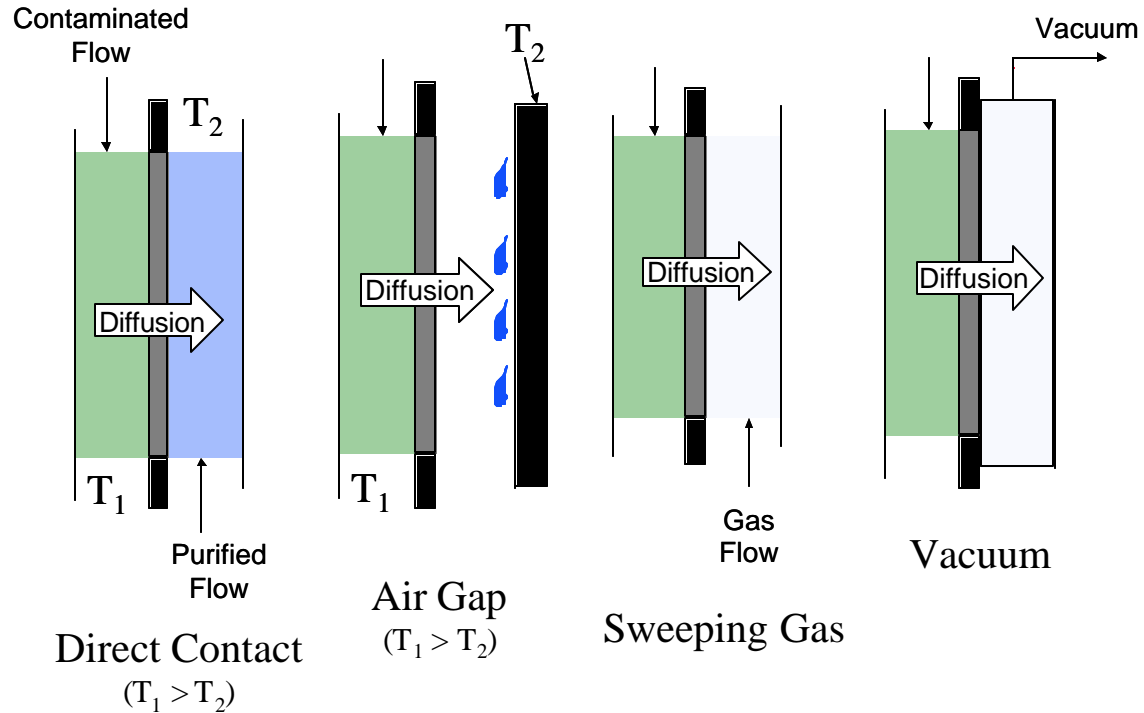


Figure 5. Methods employed in a membrane distillation scheme.

With the increasing availability of membrane technology, various forms of MD are being scrutinized for the desalination of seawater. An early study considered small scale (50 liter/day) solar-heated direct contact MD [14]. Only capital costs were reported, but Korngold et. al. suggest the system is competitive with small-scale RO [15]. Criscuoli and coworkers studied direct contact MD as an addition to RO systems to boost water recovery factors [16, 17]. Their results indicate that the addition of the MD system could increase the water recover from 40% to over 87%, but the energy cost of the process is also significantly increased (e.g. from < 18 kJ/kg fresh water to 47–54 kJ/kg), unless thermal energy for the MD system is available at no cost (< 11 kJ/kg). Product water costs were estimated as $\$1.25/\text{m}^3$ for RO and RO+MD, and $\$1.32/\text{m}^3$ for MD alone [16].

Korngold and coworkers have evaluated air-sweep pervaporation using hydrophilic membranes manufactured in their laboratories. For comparison purposes, they also report a few results achieved with a hydrophobic microporous membrane [15,18,19]. They conclude that with a feed water temperature of 60 °C (assumed to be heated at no cost), the energy requirements for feed water (neglecting costs for cooling water) and air circulation would be 7.2 kJ/kg of fresh water [15]. This figure was arrived at by assuming the pressure provided by the air circulation blower to only be 15 mm of water (0.021 psi), which appears to be a very optimistic figure (the energy cost should increase almost linearly with pressure drop).

Recently, Banat and Simandl have reported experimental results and developed a mathematical model for an air-gap MD system [20]. An economic analysis was not provided. A small commercial air-gap system manufactured by the Swedish firm SCARAB HVR was also recently tested at the University of Texas at El Paso [21, 22].

One of the modules evaluated at UTEP was previously evaluated at Sandia National Laboratories for recovering water from semiconductor manufacturing processes [22, 23]. An energy use of 158 kJ/kg product water was estimated for an air-gap MD desalination system, assuming an thermal performance ratio of 15. This value is similar to other thermally driven technologies (see Table 1).

In the present work, air sweep MD was investigated as a potentially compact process for the desalination of seawater. Since MD can produce high quality distillate at relatively low temperatures (30 to 100° C), it was anticipated that such a MD process could utilize low-grade heat industrial waste heat or a solar thermal collection system as the thermal input. The low temperature operation also offers potential advantages in terms of scale formation (calcium salts tend to be less soluble at elevated temperatures) and thus make require less pretreatment than other thermally driven methods. There may also be advantages in terms of the pretreatment required compared to pressure driven (RO) processes.

3. Hollow Fiber Membrane Contactor Evaluation

Evaluations were conducted with Celgard Liqui-Cel[®] Extra-Flow 2.5X8 membrane contactors with X-30 and X-40 hydrophobic hollow fiber membranes. These units are used commercially to add or remove dissolved gasses from liquids. Each contactor is a cylinder that is nominally 2.5” diameter and 8” in height, with an effective surface area of 1.4 m² (293 m²/m³ of volume). A schematic of the basic shell and tube contactor configuration is shown in Figure 6. Each polypropylene hollow fiber has a 300 μ O.D. The hollow fibers are bundled in a straight-through configuration inside the contactor shell. The membrane properties are summarized in Table 3.

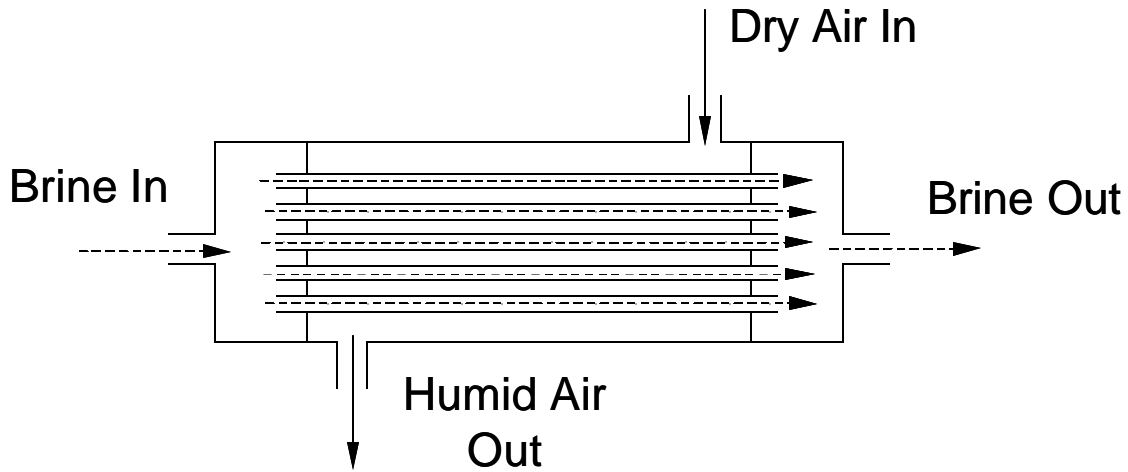


Figure 6. Schematic diagram of hollow fiber membrane cartridge with counter current sweeping gas flow.

Table 3: Celgard Liqui-Cel[®] Membrane Properties.

Unit	Max. Trans-Membrane Press./ Bubblepoint (psig)	Temperature Range (C)	Effective Pore Size (m)	Porosity (%)	Wall Thickness (m)
X-30	60/200	1-70	0.03	40	30
X-40	120/240	1-70	0.03	25	50

In the sweeping gas MD test configuration (Figure 7), heated saltwater was passed on the tube side (lumen side) of the hollow fibers with air flowing counter- or co-current to the saltwater on the shell side. In normal gas absorption or stripping applications, the liquid to be treated would be passed on the shell-side at a high flow rate, and gas (or vacuum) would be applied to the lumen side. In our case it was desirable to produce a large volume of saturated air, so air was applied to the shell side of the contactor. Air flows were measured using a calibrated rotameter and pressure was measured using a simple Bourdon gauge. In the few tests that were performed with air on the lumen side, large pressure drops were noted. A heated copper coil was used to adjust the temperature of

the house air prior to entering the contactor. Water was pumped from a stainless steel reservoir, holding approximately 4 gal, through the lumen side of the contactor with a Preston variable rate peristaltic pump. The pressure drop across the hollow fibers limited the peristaltic pump operation to a maximum water flow of 350 ml/min. The water in the reservoir was heated with a clamp-on bucket heater trimmed by a thermostatted electric immersion heater. Water evaporating on the liquid side passed through the pores and was carried away in the sweep gas. Liquid exiting the contactor was recycled back to the feed reservoir. Fresh de-ionized make-up water was occasionally added to the feed to maintain nearly constant concentrations of dissolved salts. Temperatures of the air and water flows entering and leaving the contactor were measured using type K thermocouples in contact with the flowing stream. The raw feed water inlet temperatures were set between 40 and 70 °C. Air inlet temperatures ranged from 20 to 70 °C.

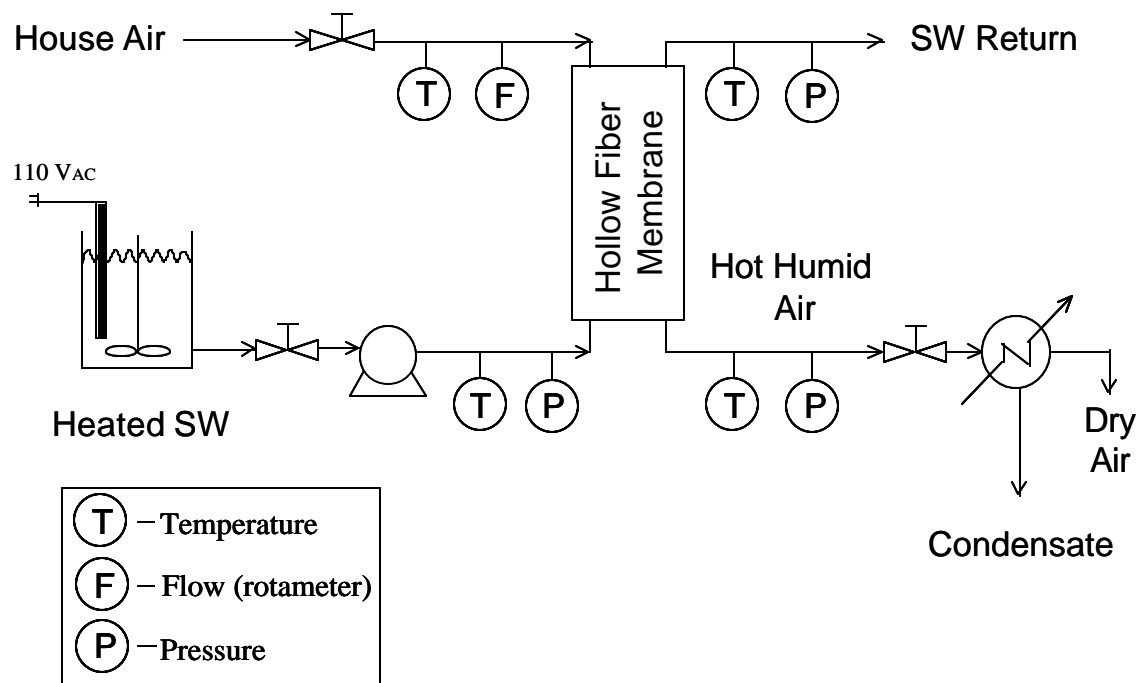


Figure 7. Schematic of the basic membrane module test setup.

In early tests, the water-saturated air exiting the contactor was passed through a conventional laboratory cold trap immersed in ice water. However, measurements of the air temperature exiting the cold trap showed that the trap was only effective in cooling the air to below room temperature at flow rates of less than 4.8 slm (0.17 scfm). Thus, these initial tests were limited to very low airflow rates. In later tests, a glycol chiller was used for condensing water from the humid air stream. In this setup the humidified air passed across cooling coils placed inside two cartridges. This arrangement provided enough cooling capacity for air flows up to 85 slm (3 scfm). In a typical test, the system was brought to a steady state (constant flows and temperatures) and then water was collected in the condensers for a period of time (typically about 1 hour) after which the

volume was measured. Several data points were usually collected at each condition to verify repeatability and steady state operation.

Our initial tests utilized an X-40 membrane cartridge that had been previously used in a different Sandia program. Prior to testing salt water, the membrane was tested by running tap water spiked with red dye through the contactor. Membrane integrity was verified as the product water was clear. Data collected for these tests is given in appendix A. Later tests used simulated seawater made by mixing commercial aquarium salts in DI water at concentrations (TDS, measured with a Myron L company AR1 conductivity meter) of 25000 ppm to 45000 ppm (usually 30000 ppm). After several runs the X-40 membrane failed and seawater passed directly into the air stream. A Celgard X-30 membrane contactor was then tested with the simulated seawater. The main difference between the X-30 and X-40 membrane is the X-40 membrane has thicker walls and fewer pores (Table 3). Figures 8 and 9 show the general trends in productivity for the X-30 and X-40 contactors. In both cases, the product water quality was very good; the TDS of the water being reduced by a factor of nearly 1000.

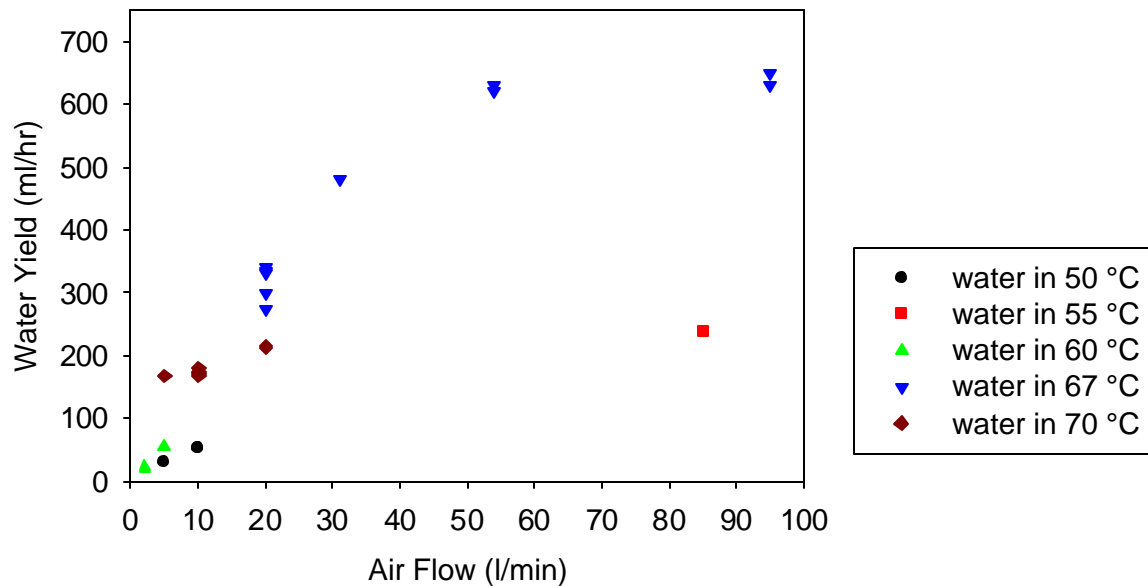


Figure 8. Water production rate as a function of airflow and water temperature for the Celgard X-30 membrane contactor. Tests conducted using saltwater at a nominal conductivity of 30,000 ppm and water flow of 300 ml/min.

As expected, Figures 8 and 9 show that increasing the water inlet temperature or the air flow increases the water collected. However, there is a limit to the effect of air flow. For the X-30 contactor, the water production rate levels off at an airflow of about 55 l/min (Figure 8). The effect is more dramatic for the X-40 contactor where the water production rate actually reaches a maximum for an air flow of about 40 slm, and then

decreases at higher flow rates. Similar effects have been reported and explained in the literature [13]. As the air flow rate increases, the boundary layer at the membrane/air interface decreases, thereby reducing the resistance to mass transfer is reduced. However, increasing the air flow also has the effect of increasing the pressure of the sweep air, which has the effect of increasing the resistance to mass transfer in the boundary. Thus, there is an optimum sweep gas flow.

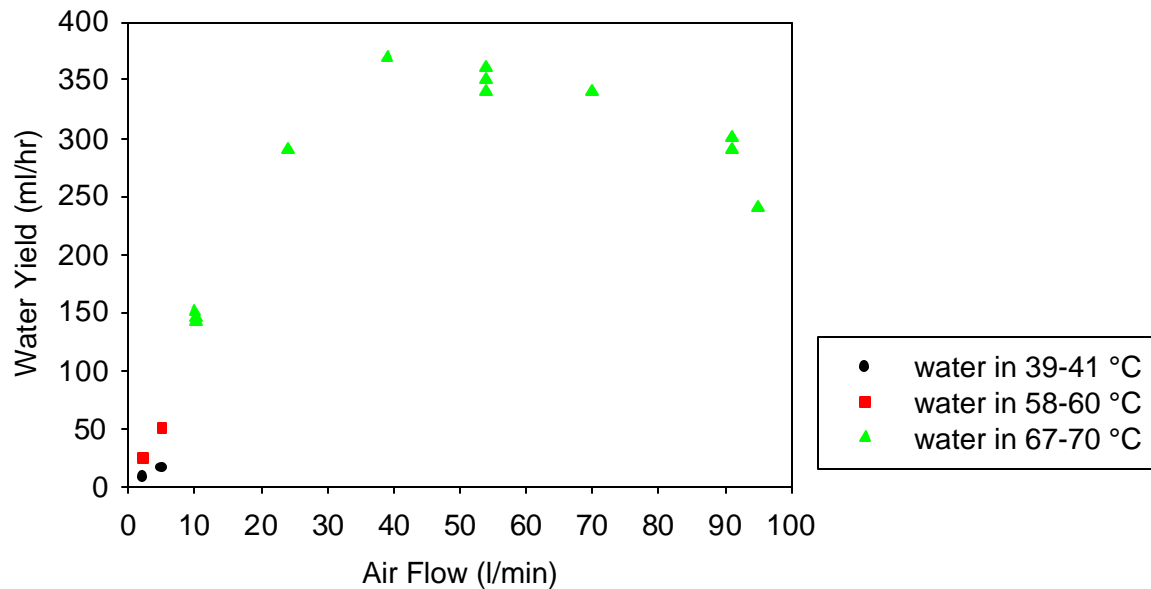


Figure 9. Water production rate as a function of airflow and water temperature for the Celgard X-40 membrane contactor. Tests conducted using saltwater at a nominal conductivity of 30,000 ppm and a water flow of 300 ml/min.

The effect of inlet air temperature on water production is shown in Figure 10 for airflow of 10 l/min (0.35 scfm) through an X-40 contactor, and for airflows of 20 – 94 l/min through an X-30 contactor. The inlet air temperature had little effect on water yield. This is consistent with the fact that the sensible heat required to raise the air temperature from ambient (20 °C) is small compared to the heat of evaporation of water, or to the heat content of the water. That is, under the conditions tested, if a cold air stream is used, the temperatures of the air stream and water stream can be equilibrated with very little drop in the water temperature (a hollow fiber membrane contactor is a very effective heat exchanger). Likewise, if a warm air stream is used, it contributes very little energy to the evaporation process.

In contrast to our results, Khayet et al. [24] reported that water flux across a hydrophobic PTFE membrane (tested in a flat plate geometry) decreased as the temperature of the sweeping gas was raised from 10 to 30 °C. They calculate that this occurred because the increase in air inlet temperature reduced the temperature difference between the hot side of the membrane (saltwater side) and the cold side (air side), resulting in a decrease in the thermally induced vapor pressure gradient across the membrane. Comparison of our results with those of Khayet et al. leads us to conclude that different combinations of flow

rates, membrane properties and geometries (and hence heat transfer properties and temperatures) can result in different operating regimes.

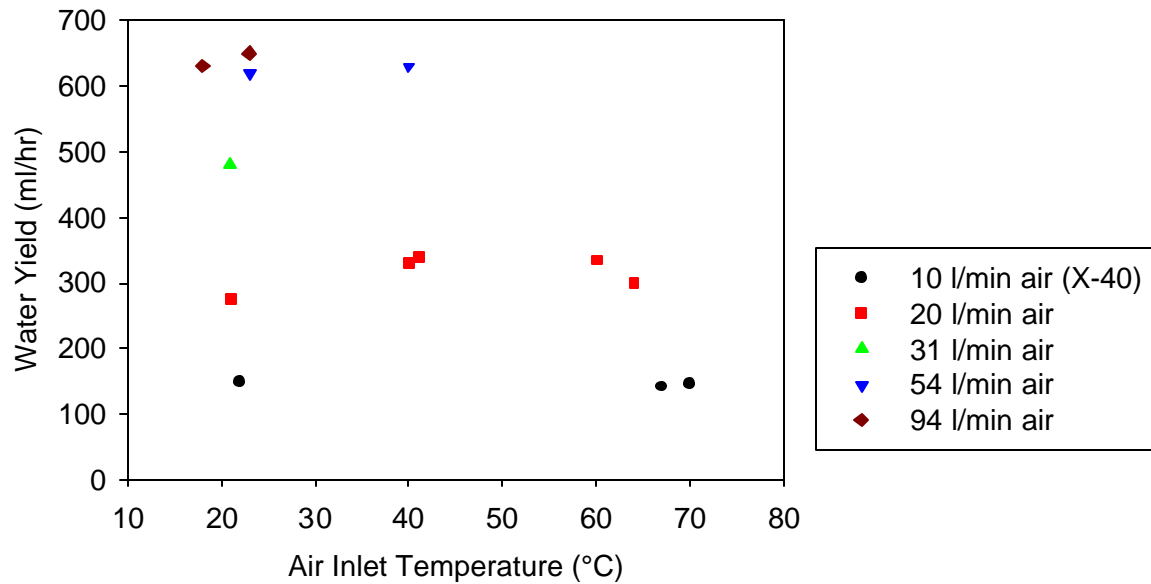


Figure 10. Effect of air inlet temperature on water yield using a Celgard X-30 (and X-40) contactor. Water flow of 300 ml/min at an inlet temperature of 67–70 °C.

For example consider a situation in which the air and water flow rates are both high relative to the flux across the membrane, the water temperature is high, the air temperature is cold, and there is no heat transfer across the membrane. In this case, the heat used for evaporation is associated entirely with the water stream, and the driving force is a vapor pressure gradient maintained by water condensing into the cold air stream. Since there is no heat transfer, and the flow rates are high, there is very little change in temperature of either stream. Clearly, in this case, an increase in the air temperature decreases the driving force across the membrane and therefore decreases the flux of water across the membrane (although the capacity of the air to hold water vapor is increased, overall the saturation humidity is still very low and contributes little to the overall water yield). This situation was approximated by the experiments of Khayet et al. wherein the flows and heat transfer were such that the air temperature remained well below the water temperature and the water temperature remained fairly constant.

Now consider a situation in which the water flow rate and temperature are low, the air flow rate and temperature are high, and there is efficient heat across the membrane. In this case, the heat for evaporation would be provided primarily by the air stream. As heat was transferred from the air stream to the water stream the temperatures would begin to equilibrate. The driving force would then be the saturation of the dry air at the equilibrium temperature. Clearly, in this case the water yield would increase with the air temperature (and flow rate). Other combinations of flows, temperatures, and heat transfer across the membrane could result in intermediate cases where the driving force is a mixture of air saturation and condensation into a cooler air stream. Being intermediate

between the two cases, the water yield will be somewhat independent of the air inlet temperature. This intermediate case appears to apply to our situation. Flows and heat transfer were such that the air temperature approached the water temperature (see Figure 11), and thus the primary (but not only) effect was the saturation of dry air.

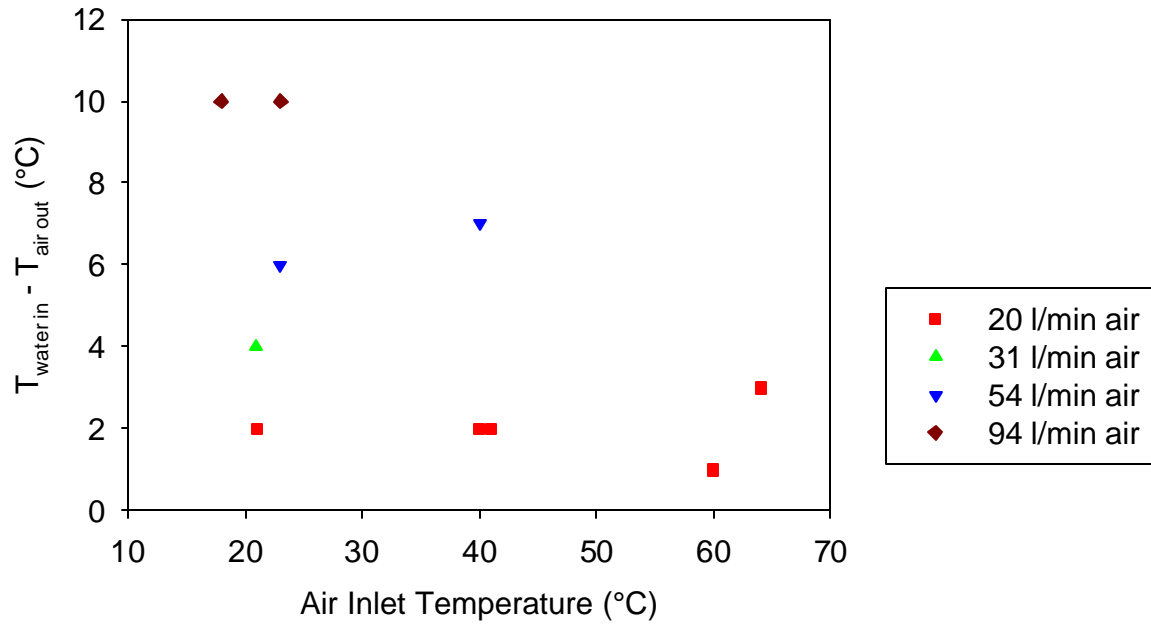


Figure 11. Data from Figure 10 (X-30 only) replotted to show that membrane contactor acts as an efficient counter-current heat exchanger. Water flow of 300 ml/min at an inlet temperature of 67-70 °C.

This point is illustrated by Figures 12-15. In these figures, the data from Figures 8 and 9 has been replotted to compare the actual water yield to that expected if the air exiting the membrane was saturated at the air exit temperature (Figure 12 and 14). Since the air temperature was by necessity measured slightly downstream from the contactor and there might have been a slight drop in air temperature, we have also compared the water yield to that expected if the air exiting the membrane was saturated at water inlet temperature (Figure 13 and 15, recall the flow is counter-current and there is efficient heat transfer across the membrane). The solid lines in the figures are representative of fully saturated air. Since much of the data lies just above the saturation line, it is clear that at the lower flow rates, most of the water exiting the membrane contactor was in the vapor phase. At high flow rates, the air remains unsaturated, and all of the product water exits the contactor in the vapor phase.

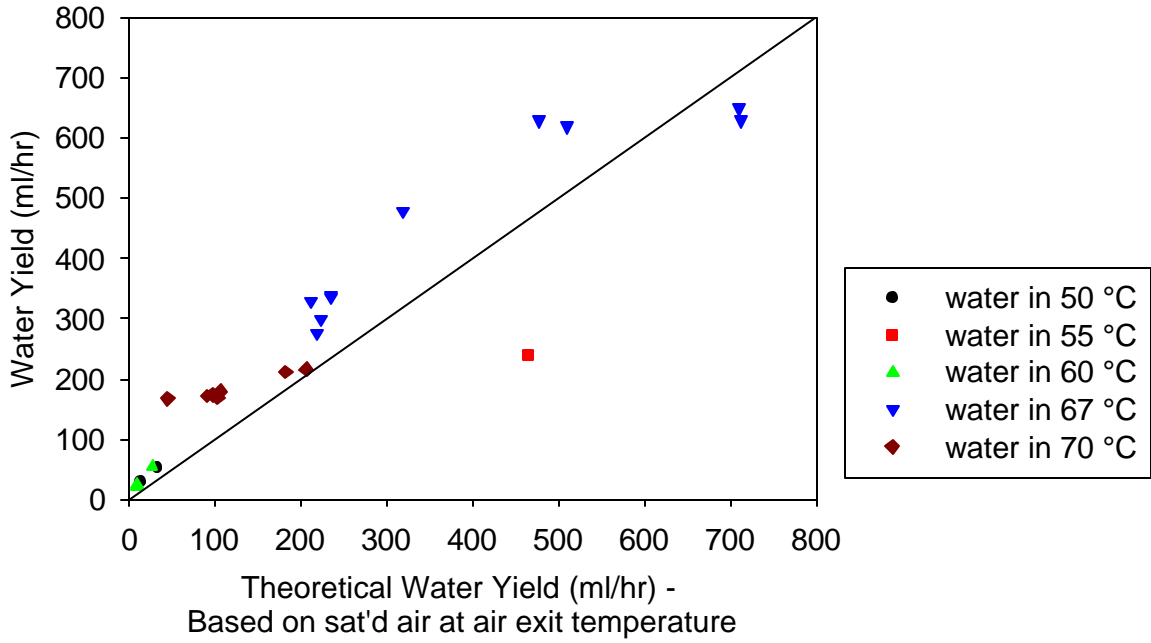


Figure 12. Water yield compared to the theoretical yield based on air saturation at the air exit temperature for the X-30 contactor.

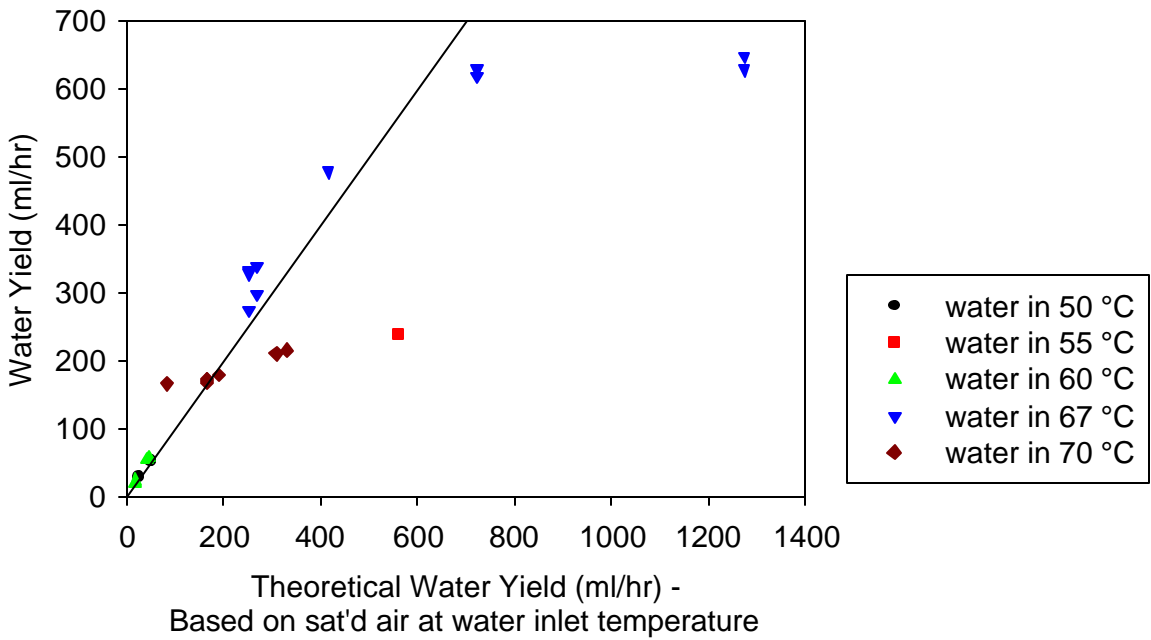


Figure 13. Water yield compared to the theoretical yield based on air saturation at the water inlet temperature for the X-30 contactor.

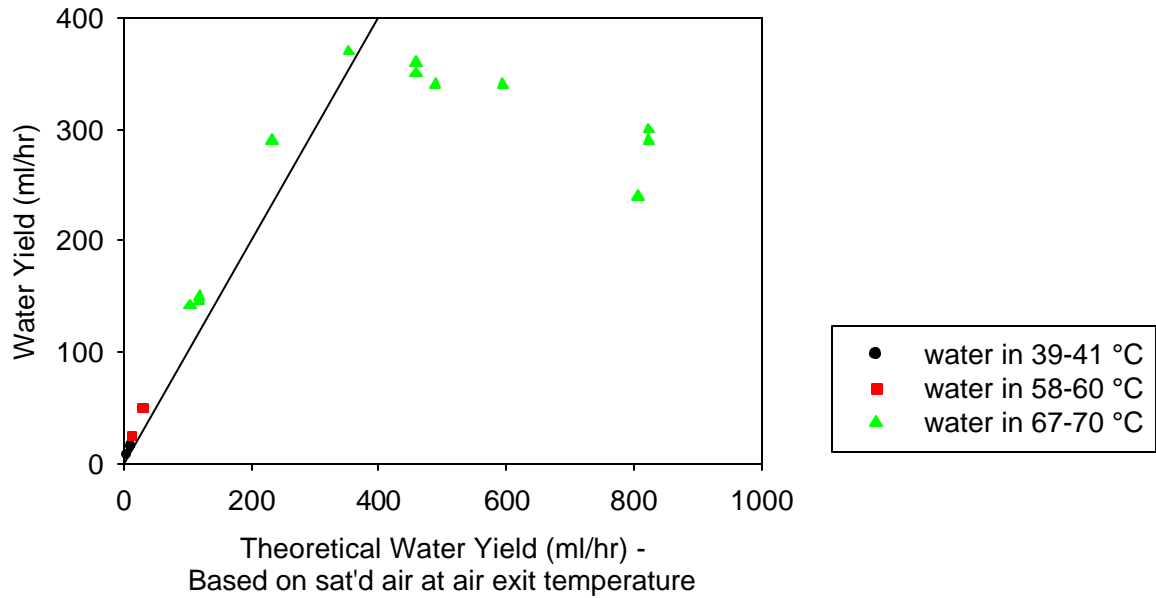
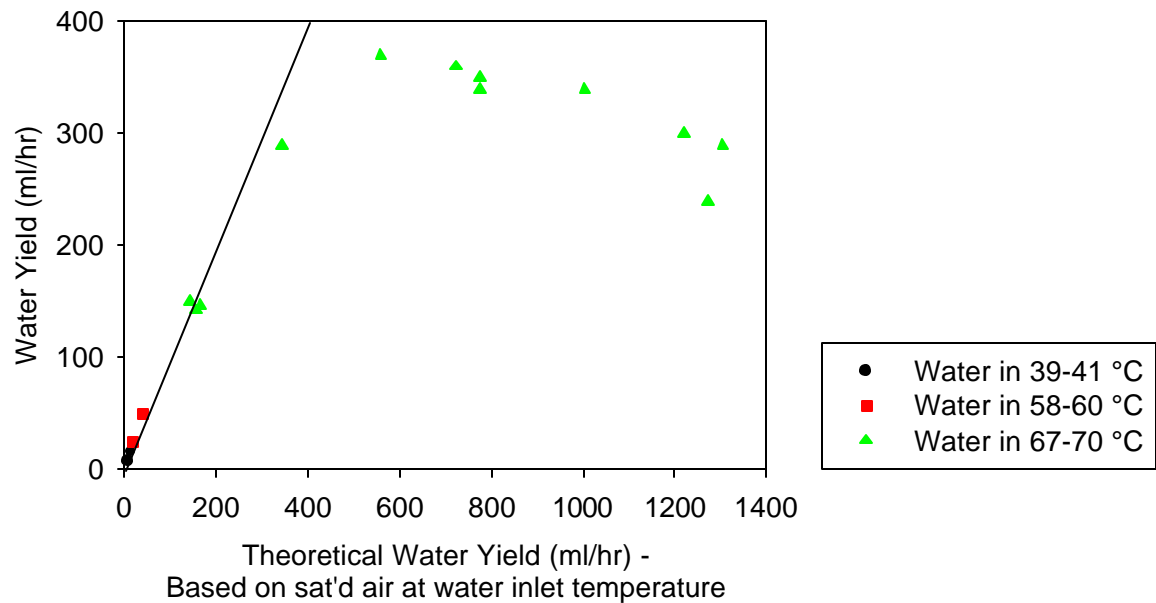


Figure 14. Water yield compared to the theoretical yield based on air saturation at the air exit temperature for the X-40 contactor.



changes in temperature in the fluids due to water evaporating and condensing are negligible. Now consider the effect of water and sweep gas temperature. If the water temperature is high, the air temperature is cold, the driving force is a vapor pressure gradient maintained as the water condenses into the cold air stream. If the air stream is cold enough, virtually all of the product water will exit the contactor as condensate, rather than as vapor saturating the sweep gas. Also, if the air side is cold enough (or the temperature gradient across the membrane is large enough), the gradient across the membrane will essentially be equal to the vapor pressure of the water on the hot liquid side, and the water yield will be limited only by the transport properties of the membrane.

Now, as the sweep gas temperature rises, an increasing fraction of the product water leaves the contactor as vapor in the sweep gas. When the temperature of the sweep gas is equal to the temperature of the feed water, there will be no condensation of water on the air side, but water will continue to cross the membrane until the sweep gas is saturated. In this case the water yield would obviously increase with the sweep gas flow. At very high flow rates, the water vapor concentration on the sweep gas side would be very low, and the same limiting case occurs wherein the gradient across the membrane is defined only by the water temperature, and the yield becomes limited by the transport properties of the membrane. Thus, from a simple flux model, there is no apparent advantage to either operating regime and one must consider the secondary effects present in real systems (geometries, boundary layers, temperature and concentration polarization, pressure drops and other energy requirements) when optimizing a system design. Equations describing heat and mass transfer in direct contact MD and vacuum MD have been developed and tested [25-31].

4. Hollow Fiber Membrane Desalination System Evaluation

Based on the information gained from initial testing, a stand-alone system was built and tested (Figure 16) with an X-40 membrane contactor. Although the X-30 contactor gave higher yields in the early evaluations, hollow fibers in the X-30 had failed shortly thereafter, and the unit was replaced with an X-40 contactor by the manufacturer. A post-mortem conducted by the manufacturer concluded that oxidative degradation of the fibers brought on by prolonged exposure to hot air probably shortened the life of the fibers. The stand-alone system design included a counter-current shell and tube heat exchanger to utilize the heat of compression from the air stream to heat the water stream. In addition to recovering the heat of compression, this arrangement prevented hot air from being fed directly to the contactor (as before, the air temperature would rise in the contactor as a result of heat transfer from the water stream). An in-line electrical heater was used to add additional heat to the water feed stream at higher flow rates. With the additional heat input, saltwater flows of up to 1000 ml/min could be heated to 70 °C.

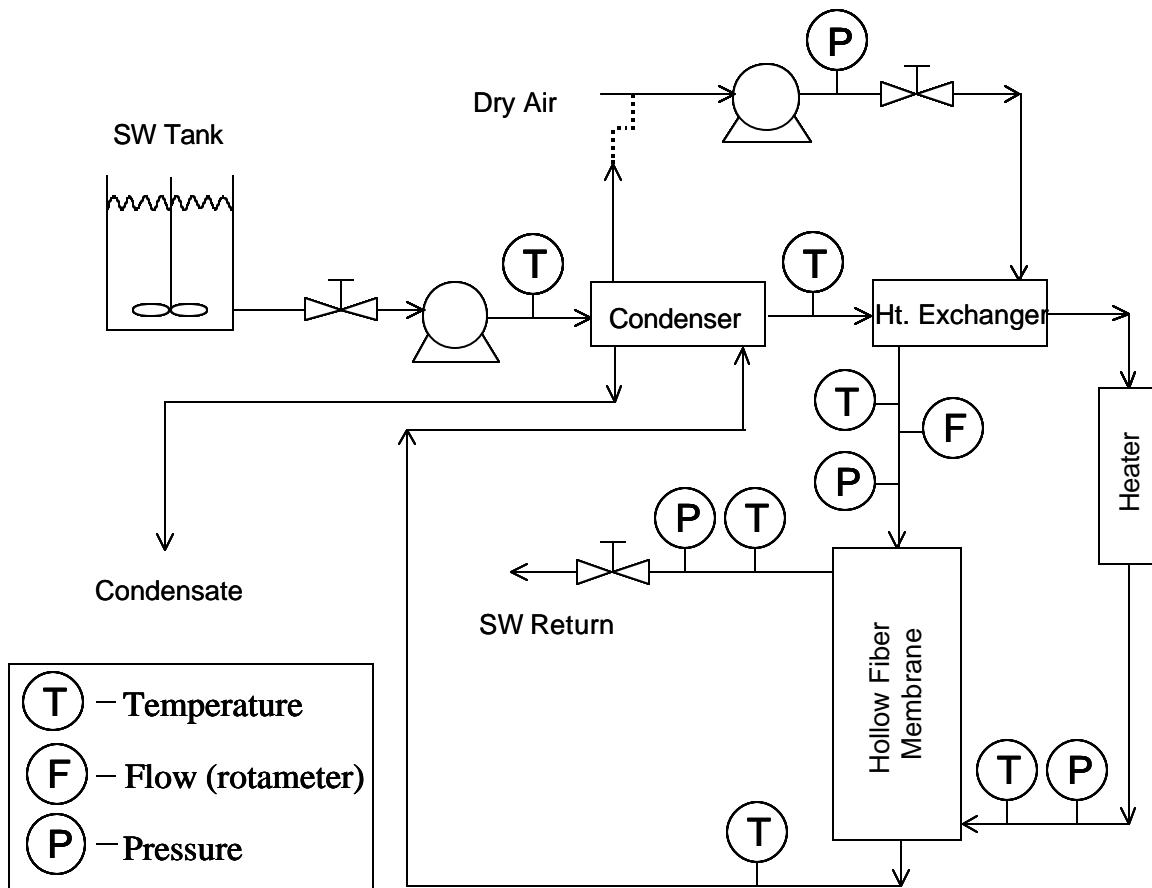


Figure 16. Schematic of the stand-alone membrane module test setup.

The saturated air leaving the membrane contactor was passed countercurrent to the entering seawater feed in a shell and tube heat exchanger, thereby cooling the air, condensing the water, and recovering some of the heat. For practical sizing reasons, the saltwater exiting the contactor was recycled to the feed tank. Deionized make-up water

was occasionally added to the feed tank to keep the salt concentration relatively constant. However, this meant that there was no continual heat reject from the system (other than parasitic losses) and thus the temperature of the feed tank slowly increased, rendering the condenser ineffective. Thus in cases where the in-line heater was used, the counter-current heat exchanger used for condensing the humidified air was replaced with the glycol chiller used in previous tests.

The initial tests of the stand alone system were conducted without the use of the in-line heater. The heated air delivered by the ¾ hp Gant compressor was capable of heating a saltwater flow of about 25ml/min to 60 °C (not all of the heat of compression could be delivered to the water since the compressor was equipped with cooling fins to prevent overheating). By varying saltwater flow through the air/water tube heat exchanger the saltwater inlet temperature to the membrane was varied between 34 and 60 °C. Under these conditions, the system was capable of producing 60 to 120 ml/hr.

The in-line heater greatly expanded the range of operating conditions and hence the water production. Airflows of up to 85 slm could be used at saltwater flow rates up to 1000 ml/min. The maximum fresh water produced was 620 ml/hr for an inlet saltwater flow of 1000 ml/min at 70 °C, and an airflow of 56 l/min. From Figure 9, we would expect that the highest yield would occur at an air flow in the range of 40–60 slm. However the 620 ml/hr produced is higher than the maximum of 370 ml/min shown in Figure 9. The reason for this can be found in Figures 14 and 15 where it is shown that at the point of maximum yield, the air flow was less than fully saturated. By increasing the water flow from 300 ml/min to 1000 ml/min, the energy available in the contactor for evaporating water and heating the air was also increased. This point is reinforced by Table 4, where it is shown that air exit temperatures increase and the drop in water temperature decreases as the water flow increases. The result of the increased energy flux into the contactor was an increase in water yield from about 45% to about 65% of theoretical (based on the water inlet temperature) under very similar conditions.

Table 4: Temperature profiles across the X-40 membrane at various air and water flows.

Saltwater Flow (ml/min)	Inlet Saltwater Temperature(C)	Outlet Water Temperature (C)	Airflow (slm)	Inlet Air Temperature (C)	Outlet Air Temperature (C)
1000	61	56	14	26	61
1000	61	56	28	26	61
1000	61	55	56.6	26	61
1000	61	53	85	26	61
1000	61	50	113	25	61
500	61	56	14	26	61
500	61	53	28	26	61
500	61	50	56.6	26	58
500	61	48	85	26	56
500	61	48	113	26	56
250	61	51	14	26	61
250	61	46	28	26	59
250	61	44	56.6	26	58
250	61	40	85	26	57
250	61	38	113	26	53

It is clear then that to achieve the maximum yield from any single contactor, two conditions must be met. First, as discussed above, the air flow should be optimized. If the air flow is too low, the air is quickly saturated (at the temperature of the water flow) and the membrane area downstream of the saturation point is unused. At very high air flows, pressure effects hinder the mass transfer and the yield decreases. Our tests indicate that the optimum air flow through an X-40 contactor is 40-60 l/min. The second condition is that the water temperature and flow rate should be as high as possible. One result of this second condition is that the temperature of the water exiting the contactor remains high. That is, much of the energy required to heat the water goes unused. One possible solution to this limitation would be to recover the energy via heat exchange with an incoming feed stream or through partial recycle (a purge stream would be necessary to limit salt accumulation). An alternate solution would be to pass the water through a series of contactors wherein the temperature would gradually reduced to an acceptably low level. A hypothetical arrangement of this type is shown in Figure 17.

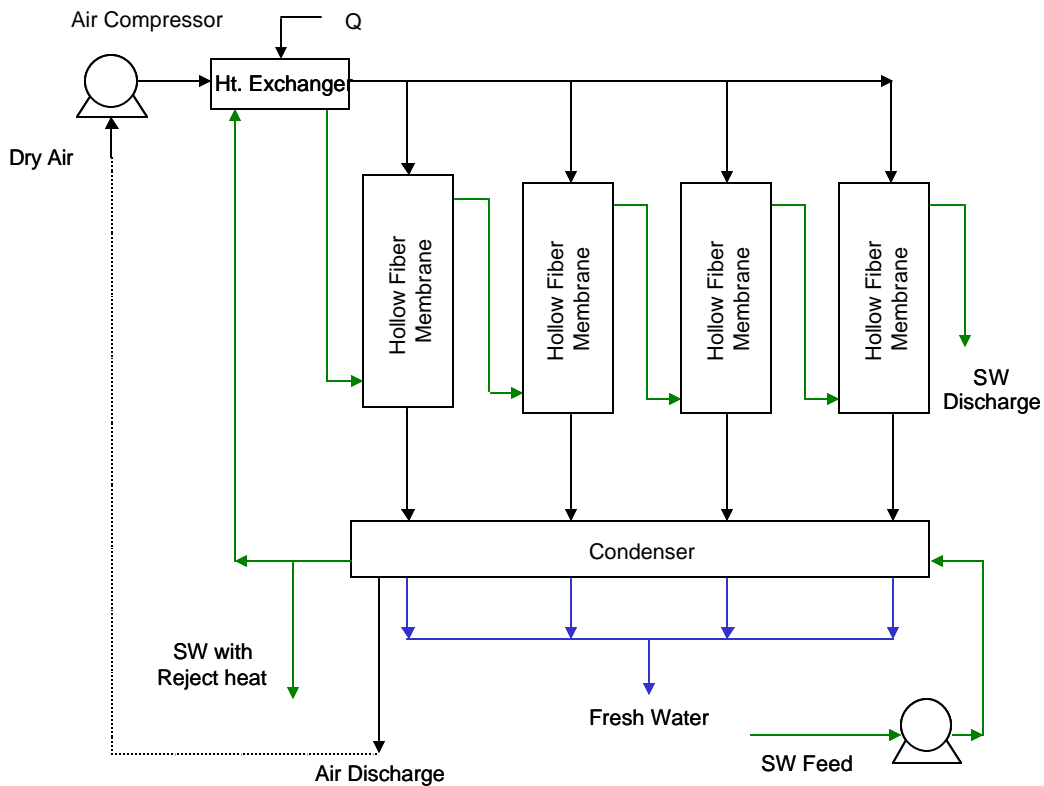


Figure 17. Schematic depiction of an MD system operating with a bank of contactors.

The system in Figure 17 is similar to our lab scale unit. A compressor circulates dry air through a number of membrane contactors. The air passes through the membranes in a parallel fashion. The salt water flow is heated by the compressed air (and additional heat input as needed) and flows through the contactors in series. The cooled, more concentrated salt water is discharged from the system. An excess of cool salt water is used to condense water from the humidified air stream. A portion of this water is then fed to the heater.

Using our single contactor system, we have simulated the operation of the system depicted in Figure 17 at a salt water flow of 1000 ml/min and at air flows of 28 and 56 l/min. This was done through a series of successive runs wherein the inlet saltwater temperature was adjusted to the outlet temperature of the previous run. The results for this exercise are shown in Table 5. A five stage system operating at a water flow of 1000 ml/min with an initial temperature of 61 °C and an air flow of 56 l/min/stage (280 l/min total) would yield almost 2 l/hr of fresh water. A four stage system with similar water flows but only half the air flow would yield only 1.1 l/hr of fresh water. This decrease is consistent with our earlier findings regarding the optimum air flow. Although additional stages could be added, it is clear that as the water temperature drops, each additional stage becomes less productive. A more productive strategy would be to increase the temperature of the water fed to the initial stages. For instance, it is estimated that raising the water feed temperature to 70 °C (the membrane temperature limit) and adding stages to achieve the same exit temperature would raise the yield to about 2.7 l/hr for an air flow of 56 l/min/stage.

Table 5. Experimental simulation of system depicted in Figure 17 with 1 l/min water flow.

Contactor Unit	Airflow (l/min)	Inlet Saltwater T(C)	Outlet Saltwater T(C)	Inlet Air T(C)	Outlet Air T(C)	Feed water Conductivity (ppm TDS)	Product water Conductivity (ppm TDS)	Product Water (ml/hr)
1	56	61	55	26	60	31000	15	480
2	56	55	50	26	55	32500	8	363
3	56	51	47	26	50	30000	7.4	287
4	56	48	44	25	46	28700	8	200
5	56	45	42	25	42	31500	5.7	165
1	28	61	57	25	61	30000	7	370
2	28	58	54	26	58	30500	6.8	310
3	28	54	51	26	55	32000	8.5	250
4	28	51	48	25	51	33000	10	210

Table 6. Thermal and saturation efficiency for system depicted in Figure 17.

Contactor Unit	Airflow (l/min)	Water Yield (ml/hr)	Theoretical (ΔT basis) (ml/hr)	Thermal Eff. (%)	Theoretical (Sat'd Air) (ml/hr)	Saturation Eff. (%)
1	56	480	638	75	526 (496)*	91 (97)
2	56	363	529	68	372 (372)	98 (98)
3	56	287	420	68	297 (281)	96 (102)
4	56	200	419	48	250 (223)	80 (90)
5	56	165	314	52	211 (178)	78 (93)
1	28	370	425	87	263	141
2	28	310	424	73	222	140
3	28	250	317	79	176	142
4	28	210	315	67	149	141

* Based on water inlet temperature. Values in parentheses based on air outlet temperature.

The efficiency of the multi-stage process is examined in Table 6. The thermal efficiency of each stage was determined by comparing the actual water yield to that possible if all the enthalpy change of the water (based on the temperature drop) was used to evaporate water at the average temperature of each stage. The saturation efficiency was calculated by comparing the actual water yield to that expected if the water exiting each stage was saturated at the water inlet temperature (or air outlet temperature for the higher flow rate, in parentheses). As might be expected from our earlier results, Table 6 shows that at the higher air flow, the air is just less than fully saturated with water (the air flow is near the optimum). At the lower air flow, the water yields exceed those expected from saturating the air stream (the system is air flow limited). Again this is consistent with our previous results, although the 40% excess water is surprisingly high. As noted before, however, the overall product water yields are better for the higher (and close to optimum) air flow.

The results for the thermal efficiency are less straightforward. At best, only 87% of the energy lost by the water stream is used for evaporation. A portion of this “lost” energy is associated with heating the air stream (up to 10% for the high air flow and 5% for the lower air flow). The remainder must be associated with parasitic losses, e.g. heat transfer to the environment. Much of this could probably be prevented through better insulation of the system. One puzzling aspect of the data is the fact that the thermal efficiency decreases as the temperature decreases. Since the rate of heat transfer (and hence energy loss to the environment) generally increases with temperature gradient, this trend is unexpected and currently unexplained. It may be related to the different effects of temperature on heat transfer and mass transfer (evaporation).

It is important to note that even if the thermal efficiency of the system were brought to 100%, thermal energy utilization would be sub-par compared to conventional thermal desalination processes. This is because the large scale technologies recover the heat of vaporization fairly efficiently by using the heat of condensation of the saturated steam to drive evaporation in a successive stage (see section 1 of this report). In a sweeping gas system, only a small fraction of the gas stream leaving the contactor is water vapor and the amount of water that can be recovered by an incremental change in temperature is also relatively small. Thus, the temperature of the air stream must be brought quite low in order to recover significant amounts of water, making it difficult to recover the heat in a useful form. The “dewvaporation” process developed at the university of Arizona [32] addresses this problem by passing the humidified air across the back of the falling film evaporator. A similar approach has been developed and termed mechanically intensified evaporation (MIE) [33]. This approach could only be applied to MD if a new contactor configuration was developed.

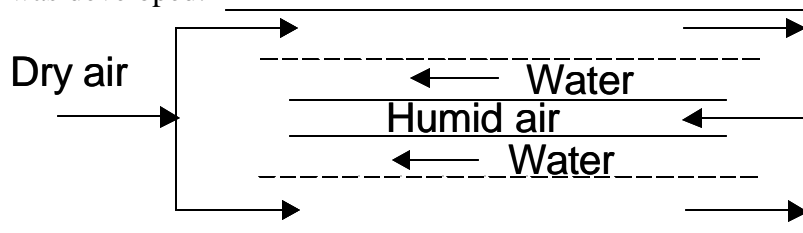


Figure 18. Proposed scheme for more efficient heat utilization in sweeping gas MD.

For example, this new configuration might use a solid walled hollow fiber located inside of a microporous hollow fiber that in turn was inside a shell as shown in Figure 18. Dry air would flow in the shell surrounding the hollow fibers and be humidified by the water passing through the annulus of between the fiber walls. The humidified air stream (possibly with additional heat added) would be then directed back through the inner fiber where it would return the heat of evaporation to the water stream thereby condensing the product water. In general however, until new contactor arrangements are developed, it appears that a sweeping gas MD system would likely need access to low grade, low cost waste heat in order to be economically viable.

Assuming that heat recovery is improved, or that waste heat is available at zero or very low cost, the next consideration is the air flow. The volume of air required to produce a significant amount of water is very large, and the costs associated with moving this air could be considerable [34]. In order to minimize these costs, a system would need to operate at as high a temperature, and with as low a pressure drop as possible. Figure 19 illustrates the strong effect of temperature on the water content of saturated air, and hence the importance of operating temperature. The saturation humidity roughly doubles for every 10 °C increase in temperature. Air at 90 °C can hold five times more water than air at 70 °C (the limit of the Celgard membranes).

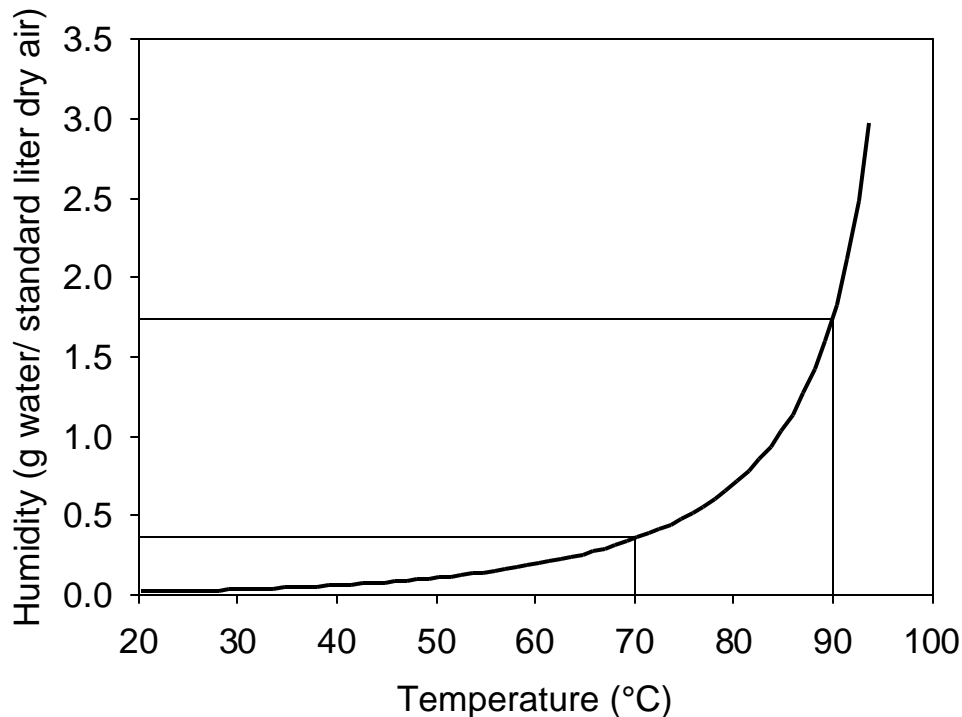


Figure 19. Saturation humidity of air as a function of temperature – adapted from “Perry’s Chemical Engineering Handbook, 6th edition”.

The system design shown in Figure 18 was aimed at maximum heat utilization. Figure 20 shows a variation of the design in Figure 18 that is aimed at minimizing the air flow. In this design heat is added to the water between each contactor stage so that the air

leaving each stage is saturated at as high a temperature as possible (the limit of the contactor). As before, heat could be recovered from the concentrated brine leaving the final stage by counter-current exchange with the fresh salt water feed. For a system of this type, the total yield would vary linearly with the number of stages. A five stage system operating at 70 °C, 1000 ml/hr water and an air flow of 56 l/min/stage would produce 4 l/hr of water. Similarly a five stage system operating at 61 °C, 1000 ml/hr and 56 l/min/stage would produce 2.4 l/hr (compared to about 2 l/hr without interstage heating, see above).

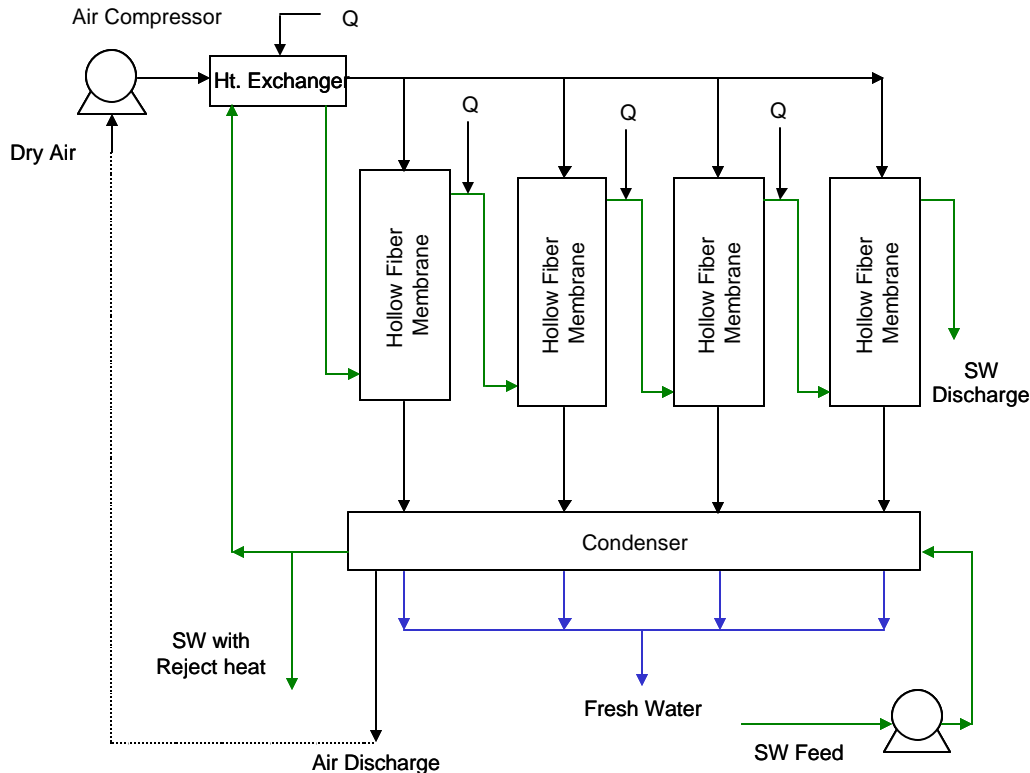


Figure 20. Multicontactor configuration for minimizing air flow requirements.

In Table 7 we have tabulated the minimum total air flows required to produce 1000 gal/day of fresh water as a function of water temperature for a system of the type shown in Figure 20 (fully saturated air in each exiting each stage). If one accounts for the capacity of the cool air to condense water (i.e. if there is no heat transfer across the membrane) as well as the saturation capacity, the required air flows are only slightly reduced (<10%). Table 7 also includes estimates of energy requirements and operating costs (assuming \$0.10/kWhr) associated with the blower operation. The horsepower requirements are based on typical low-pressure blowers operating at maximum pressure of 0.068 to 0.14 atm (1-2 psi). In our experiments with hollow fiber cartridges, pressure drops were actually higher than this assumed value and thus operation costs would be proportionally higher. The pressure requirements could possibly be decreased by redesigning a membrane contactor. However the end product would likely negate one the advantages of using hollow fibers, namely compactness.

A comparison of the costs in Table 7 with those in Table 2, illustrates that the high air flow requirements is one of the principal reasons that sweeping gas MD is unlikely to be ever be a competitive technology for desalination. At all but the highest temperatures (which are above the limit for many membranes), the costs of operating the blower alone is greater than the cost of producing water with currently available technology. Even if the cost of power is only \$0.05/kWhr (a more realistic estimate of current costs) and heat utilization is greatly improved, the potential savings are probably not enough to justify the development required to bring this technology to market. This is particularly true when one adds the capital costs of the units, the additional operating costs such as power to circulate water through the system, the cost of pretreating the raw seawater being fed to the unit (at a minimum filtration would be required), and the cost of disposing of the product brine.

Table 7. Approximate operating costs for low-pressure air blowers used in a 1000 gallon/day sweep gas MD system (\$0.10/kWhr basis).

Saturated Air Temp °C	Humidity gal H ₂ O/sl air	Airflow sl/min	Blower Size hp	Energy kWhr	Cost \$/m ³ (\$/1000 gal)
60	.000051	13,511	18	322	8.50 (32.20)
70 <i>Celgard limit</i>	.000093	7,440	10	179	4.70 (17.90)
80	.00018	3,774	2.5	45	1.20 (4.50)
90	.00047	1,491	1	18	0.50 (1.80)

5. Conclusions and Recommendations

Air sweep membrane desalination systems are capable of producing low total dissolved solids (TDS) water, typically 10 ppm or less, from seawater, using low grade heat. However, there are several barriers that currently prevent sweeping gas MD from being a viable technology. The primary problem is that large air flows are required to achieve significant water yields, and the costs associated with moving these large volumes of air through a confined space are prohibitive. A related barrier is the temperature limitations of current hydrophobic microporous membranes. The air flow requirement is strongly dependent on the system operating temperature, and can be roughly halved for each 10 °C increase in operating temperature. The temperature limit of the membranes used in this study was 70 °C. Higher flux membranes tend to have even more restrictive temperature limits. In situations of long term use, oxidative degradation of the membrane due to continuous contact with hot air may also be an issue. At least one of the membrane failures that occurred during the course of this study may have resulted from oxidation.

One possible advantage of a sweeping gas MD system is that it could utilize low grade waste heat to produce fresh water (provided air flow could also be economically provided). In fact, this is almost a necessity since heat utilization and recovery in sweeping gas MD is not very efficient, especially when compared to current large scale desalination technologies. The reason for this poor heat utilization is that the humidified air stream must be cooled to a relatively low temperature in order to recover a large fraction of the water from the humidified air. This fact, coupled with the shell and tube geometry of a hollow fiber contactor, means that the heat of evaporation is rejected from the system in an unusable form.

If sweeping gas membrane distillation is ever to compete economically with established technologies, new and different contactor geometries are necessary. These designs must achieve efficient contact with an extremely low pressure drop. Furthermore the temperature limits of the system must be improved. Both of these improvements are necessary to minimize the costs associated with air flow through the system. In addition, a method of coupling water condensation with evaporation (e.g. in a secondary stage) for heat recovery must be developed if the technology is to be decoupled from a low-grade inexpensive heat source. The designs must also limit the degree of pretreatment required for the raw water feed. Hollow fiber systems generally require feeds that are very free from particulates to avoid pore plugging. In our work, localized precipitation of salts in the pores required that the contactors be frequently cleaned, even though the salt concentration fed to the contactor was kept almost constant. This problem would also need to be addressed or allowed for in the design.

Rather than focus on these improvements, a more productive route may be to investigate the integration of a membrane system with a mechanical vapor compression cycle. This arrangement should have advantages over the sweeping gas system in that vacuum operation eliminates the cost of circulating air in the system (only water vapor would be transported). Furthermore, heat recovery should be improved since the recovery of liquid water from a vapor (steam) stream requires a smaller temperature drop than is practically required for a saturated air stream (a condensing vapor stream can drive an evaporation

step at almost the same temperature). Finally the membrane system may have advantages in terms of mist elimination compared to conventional MVC.

Acknowledgement: The authors would like to acknowledge the efforts of Shawn Begay who collected some of the data presented in this report. The authors also gratefully acknowledge Maher Tadros and the Advanced Concepts Group (ACG) for their support and funding of this work.

References

1. G.F. Leitner, *Int. Desalination and Water Reuse Quart.* 7 (1998) 10.
2. R. Engelman, R.P. Cincotta, B. Dye, T. Gardner-Outlaw, J. Wisnewski "People in the Balance: Population and Natural Resources at the Turn of the Millennium" Population Action International, Washington, D.C. (2000).
3. H.M. Ettouney, H.T. El-Dessouky, I. Alatiqi, *Chemical Engineering Progress*, September 1999, 43.
4. M.A. Darwish, N.M. Al-Najem, *Applied Thermal Engineering* 20 (2000) 399.
5. R. Semiat, *Water International* 25 (2000) 54.
6. K.S. Speigler and Y.M. El-Sayed, *A Desalination Primer*, Balaban Desalination Publications, Santa Maria Imbaro, Italy (1994).
7. H.T. El-Dessouky, H.M. Ettouney, Y. Al-Roumi, *Chemical Engineering Journal* 73 (1999) 173.
8. J. DeGunzbourg, D. Larger, *Int. Desalination and Water Reuse Quart.* 7 (1998) 15.
9. O.K. Buros, "The ABCs of Desalting, Second ed." International Desalination Association, Topsfield, Mass, 2000.
10. S.L. Postel, G.C. Daily, P.R. Ehrlich, *Science* 271 (1996) 785.
11. S.L. Gillett, *Nanotechnology* 7 (1996) 177.
12. C.A. Smolders and A.C.M. Franken, *Desalination* 72 (1989) 249.
13. K.W. Lawson and D.R. Lloyd, *J. Membr. Sci.* 124 (1997) 1.
14. P.A. Hogan, A.G. Sudito, A.G. Fane, G.L. Morrison, *Desalination* 84 (1991) 123.
15. E. Korngold, E. Korin, I. Ladizhensky, *Desalination* 107 (1996) 121.
16. E. Drioli, F. Lagana, A. Criscuoli, G. Barbieri, *Desalination* 122 (1999) 141.
17. A. Criscuoli, E. Drioli, *Desalination* 124 (1999) 243.
18. E. Korngold and E. Korin, *Desalination* 91 (1993) 187.
19. E. Korin, I. Ladizhensky, E. Korngold, *Chemical Engineering and Processing* 35 (1996) 451.
20. F.A. Banat and J. Simandl, *Separation Science and Technology* 33 (1998) 201.
21. S. Solis "Water Desalination by Membrane Distillation Coupled with a Solar Pond" Masters Thesis, Dept. of Civil Engineering, University of Texas at El Paso, 1999.
22. *Dr. John Walton, UTEP, personal communication.*
23. *Robert Donovan, SNL, personal communication.*
24. M. Khayet, P. Godino, J.I. Mengual, *J. of Membrane Science* 165 (2000) 261.
25. R.W. Schofield, A.G. Fane, C.J.D. Fell, *J. of Membrane Science* 33 (1987) 299.
26. R.W. Schofield, A.G. Fane, C.J.D. Fell, *J. of Membrane Science* 53 (1990) 159.
27. R.W. Schofield, A.G. Fane, C.J.D. Fell, *J. of Membrane Science* 53 (1990) 173.
28. S. Bandini, G.C. Sarti, C. Gostoli, *Proc. of the Third Int. Conf. on Pervaporation Processes in the Chemical Industry*, Nancy, France (1988) 117.

29. S. Bandini, C. Gostoli, G.C. Sarti, *J. of Membrane Science* 73 (1992) 217.
30. A. Saavedra, S. Bandidni, G.C. Sarti, *Proc. of the Euromembrane Conf., Paris, France* (1992) 199.
31. G.C Sarti, C. Gostoli, S. Bandini, *J. of Membrane Science* 80 (1993) 21.
32. J.R. Beckman, Final Report "Innovative Atmospheric Pressure Desalination" U.S. Dept. of the Interior, Bureau of Reclamation, Agreement Number 98-FC-81-0049, (1999).
33. M. Vlachogiannis, V. Bontozoglou, C. Georgalas, G. Litinas, *Desalination* 122 (1999) 35.
34. A.A.M. Sayich, Solar Energy Engineering, Academic Press, London, 1977.

DISTRIBUTION:

10 MS 1349 James Miller, 1846
5 MS 1349 Lindsey Evans, 1846
5 MS 0839 Maher Tadros, 16000
1 MS 9403 Bob Bradshaw, 8722
1 MS 0892 Steve Showalter, 1764
1 MS 0706 Tom Hinkebein, 6113
1 MS 0755 Mike Hightower, 6251
1 MS 0755 Tina Nenoff, 6233
1 MS 0759 Jim Krumhansl, 6118
1 MS 1411 Jim Voigt, 1846
1 MS 1411 B.G. Potter, 1846
1 MS 0755 Dan Horschel, 6233
1 MS 0701 Wendy Cieslak, 6100
1 MS 9018 Central Technical Files, 8945-1
2 MS 0899 Technical Library, 9616
1 MS 0612 Review and Approval Desk, 9612
For DOE/OSTI